is actually Ni(II) with a $d_{x^2-y^2}$ electron antiferromagnetically coupled to a ligand thiyl radical.[18] In this event, major changes in Ni-S distances (0.14 Å, Table IV) would not occur, especially when the radical center is likely to be delocalized over most or all sulfur atoms.

In ongoing work, we are examining further combinations of thiolate, amidate, and oximate ligands in chelate ring structures of different sizes as means of modulating the stability of Ni(III) and obtaining systems with hydrogenase reactivity.

Acknowledgment. This research was supported by NSF Grants CHE 85-21365 and CHE 89-03283. X-ray diffraction equipment was obtained by NIH Grant 1 S10 RR 02247. We thank Prof. R. A. Scott for communication of unpublished results.

Supplementary Material Available: Crystallographic data for and details of data collections, thermal and positional parameters, interatomic distances and angles, and calculated hydrogen atom positional parameters for $(Et_4N)_2[Ni(pdtc)_2]$, $(Ph_3PCH_2Ph)[Ni(pdtc)_2]$, and $(Ph_3PCH_2Ph)[Co(pdtc)_2]$ (24 pages); calculated and observed structure factors (79 pages). Ordering information is given on any current masthead page.

Formation and Structure of Alkyl Peroxide Complexes of Germanium(IV) Porphyrins from Direct Reactions with Alkyl Hydroperoxides and by Photolysis of Alkylgermanium(IV) Porphyrins in the Presence of Dioxygen

Alan L. Balch,* Charles R. Cornman, and Marilyn M. Olmstead

Contribution from the Department of Chemistry, University of California, Davis, California 95616. *Received July 13, 1989*

Abstract: $TPPGe(OOCH_2CH_3)_2$ (TPP is the dianion of tetraphenylporphyrin) which has remarkable thermal stability but is hydrolytically sensitive has been prepared by both reaction of ethyl hydroperoxide with $TPPGe(OH)_2$ and by photolysis of $TPPGe(CH_2CH_3)_2$ in the presence of dioxygen. The latter reaction involves successive reactions of the two ethyl groups to give $TPPGe(OOCH_2CH_3)(CH_2CH_3)$ and $TPPGe(OOCH_2CH_3)_2$ and the decomposition/hydrolysis products $TPPGe(OH)(CH_2CH_3)$ and $TPPGe(OH)(OOCH_2CH_3)$. X-ray diffraction studies on both $TPPGe(OOCH_2CH_3)_2$ and $TPPGe(OCH_2CH_3)_2$ confirm their similar, six-coordinate structures. The ring current shifted ^1H NMR resonances of the axial ligands in these complexes are more effective than electronic spectra in monitoring reaction products. Photolysis of $TPPGe(OOCH_2CH_3)_2$ in toluene produces acetaldehyde and ethanol in ratios that are highly temperature dependent. At 23 °C the acetaldehyde/ethanol ratio is 0.55, while at −70 °C it is 3.5.

Recently we have shown that dioxygen reacts with paramagnetic ($S = 1/2$) $PFe^{III}CH_2CH_3$ (P is a tetrarylporphyrin dianion) at −80 °C in toluene solution to form a high spin ($S = 5/2$) alkylperoxo complex (eq 1).[1-4] This intermediate has very little stability and subsequently decomposes even at −80 °C into acetaldehyde and the hydroxy complex $PFe^{III}OH$ (eq 2). Depending on the size of the substituents on the meso phenyl groups of the porphyrin, $PFe^{III}OH$ may then undergo dehydration to form $PFe^{III}OFe^{III}P$ (eq 3).

$$PFe^{III}CH_2CH_3 + O_2 \rightarrow PFe^{III}OOCH_2CH_3 \quad (1)$$

$$PFe^{III}OOCH_2CH_3 \rightarrow PFe^{III}OH + O{=}CHCH_3 \quad (2)$$

$$2PFe^{III}OH \rightarrow PFe^{III}OFe^{III}P + H_2O \quad (3)$$

In toluene $TMPFe^{III}OH$ (TMP is the dianion of tetramesitylporphyrin) catalyzes the decomposition of ethyl hydroperoxide with the formation of acetaldehyde and smaller amounts of ethanol.[3] The formation of acetaldehyde presumably occurs through the two-step mechanism given in eqs 4 and 5. While it has been possible to detect the paramagnetic, five-coordinate intermediate $PFe^{III}OOR$ in these studies, this species is clearly too reactive to allow for its isolation and detailed structural characterization.

$$CH_2CH_3OOH + TMPFe^{III}OH \rightarrow TMPFe^{III}OOCH_2CH_3 + H_2O \quad (4)$$

$$TMPFe^{III}OOCH_2CH_3 \rightarrow TMPFe^{III}OH + O{=}CHCH_3 \quad (5)$$

In view of the significance of this work to diverse fields including dioxygen activation,[5] enzymatic hydroperoxide decomposition,[6] the synthetic utility of Fe-C bonds,[7] and the behavior of iron-containing oxygenases,[8] we have undertaken to establish the viability of the steps involved in eq 1-5 in a system in which the alkyl peroxide complex is sufficiently stable to isolate. Since it is likely that the decomposition of $PFe^{III}OOCH_2CH_3$ involves cleavage of the O-O bond to form intermediates in higher oxidation states (e.g., $PFe^{IV}{=}O$ or $(P^{\bullet})Fe^{IV}{=}O^+$ where $(P^{\bullet})$ is a porphyrin radical monoanion), it should be possible to obtain and isolate complexes containing an $M-OOCH_2CH_3$ unit by utilizing

(1) Arasasingham, R. D.; Balch, A. L.; Latos-Grazynski, L. *J. Am. Chem. Soc.* **1987**, *109*, 5846.
(2) Arasasingham, R. D.; Balch, A. L.; Latos-Grazynski, L. Studies in Organic Chemistry 33. In *The Role of Oxygen in Chemistry and Biochemistry*; Ando, W.; Moro-Oka, Y.; Eds.; Elsevier: New York, 1988; p 417.
(3) Arasasingham, R. D.; Balch, A. L.; Cornman, C. R.; Latos-Grazynski, L. *J. Am. Chem. Soc.* **1989**, *111*, 4357.
(4) Arasasingham, R. D.; Cornman, C. R.; Balch, A. L. *J. Am. Chem. Soc.* **1989**, *111*, 7800.
(5) *Metal Ion Activation of Dioxygen*; Spiro, T. G., Ed.; Wiley-Interscience: New York, 1980. Sheldon, R. A., Kochi, J. K. *Metal-Catalyzed Oxidations of Organic Compounds*; Academic Press: New York, 1981.
(6) Marnett, L. J.; Weller, P.; Battista, J. R. In *Cytochrome-P450: Structure, Mechanism and Biochemistry*; Ortiz de Montellano, P. R., Ed.; Plenum Press: New York, 1986; p 29.
(7) Corey, E. J.; Nagata, R. *J. Am. Chem. Soc.* **1987**, *109*, 8107. Corey, E. J.; Walker, J. C. *J. Am. Chem. Soc.* **1987**, *109*, 8168.
(8) *Molecular Mechanisms of Oxygen Activation*; Hayaishi, O.; Ed.; Academic Press: New York, 1974. Ortiz de Montellano, P. R. *Cytochrome P-450*; Plenum Press: New York, 1986.

0002-7863/90/1512-2963$02.50/0

Table I. ^{1}H NMR Resonances of TPPGe(X)Y in Benzene-d_6 Solution

compound TPPGe(X)Y	axial ligand: pyrrole δ (ppm)	X δ (ppm)	J (Hz)	Y δ (ppm)	J (Hz)
TPPGe(Cl)Cl	8.99				
TPPGe(Et)Et	9.02	−4.09 (t) −6.43 (q)	7.9	X = Y	
TPPGe(OOEt)Et	9.03	−1.19 (t) 0.30 (q)	6.9	−3.82 (t) −5.92 (q)	7.9
TPPGe(OH)Et	9.02	not obsd		−3.93 (t) −6.08 (q)	7.9
TPPGe(OH)OOEt	9.03	not obsd		−0.13 (q) −1.14 (t)	7.0
TPPGe(OOEt)OOEt	9.05	−0.04 (q) −1.11 (t)	6.9	X = Y	
TPPGe(OH)OH[a]	9.049	−6.98		X = Y	
TPPGe(OEt)OEt	9.01	−1.94 (t) −2.27 (q)	6.9	X = Y	
TPPGe(Cl)Et	9.03			3.81 −5.78 (q)	6.6
TPPGe(OOH)Et	9.03	not obsd		−3.85 (t) −5.94 (q)	7.9
TPPGe(O-t-Bu)$_2$	9.00	−2.33		X = Y	
TPPGe(OO-t-Bu)$_2$	9.04	−1.34		X = Y	

[a] In $CDCl_3$.

as M those metal ions which cannot undergo further oxidation.

Relatively few complexes of alkyl peroxides have been structurally characterized.[9] None of these have, as yet, involved a porphyrin ligand. Moreover, metalloporphyrins are known to undergo modification (bleaching) when exposed to alkyl peroxides.[10]

The present studies have concentrated on main group ions, particularly Ge^{IV}. This was done partly because of earlier reports that photolysis of $PGe^{IV}R_2$ in the presence of dioxygen gave evidence for the formation of PGeR(OOR) and $PGe(OOR)_2$.[11] However, there was some question in our minds as to the ability of that investigation to differentiate between peroxide and alkoxide as possible products. This differentiation is particularly important since there are many examples of oxygenation of metal–carbon bonds that give alkoxide complexes as the products.[12]

Results

Preparation of $TPPGe(OOCH_2CH_3)_2$ and Comparison with $TPPGeX_2$ (X = OH, OCH_2CH_3, CH_2CH_3). Samples of $TPPGeX_2$ (X = Cl, OH, or CH_2CH_3) were prepared via the methods of Maskasky and Kenney.[13] $TPPGe(OCH_2CH_3)_2$ was obtained by treating $TPPGeCl_2$ with lithium ethoxide (sodium ethoxide does not work). $TPPGe(OCMe_3)_2$ was obtained similarly. Exchange reactions between $TPPGe(OH)_2$ and protic substances, ROH, are governed by the acidity of ROH. Those more acidic than water, including phenols, acetic acids, and alkylperoxides, react to form

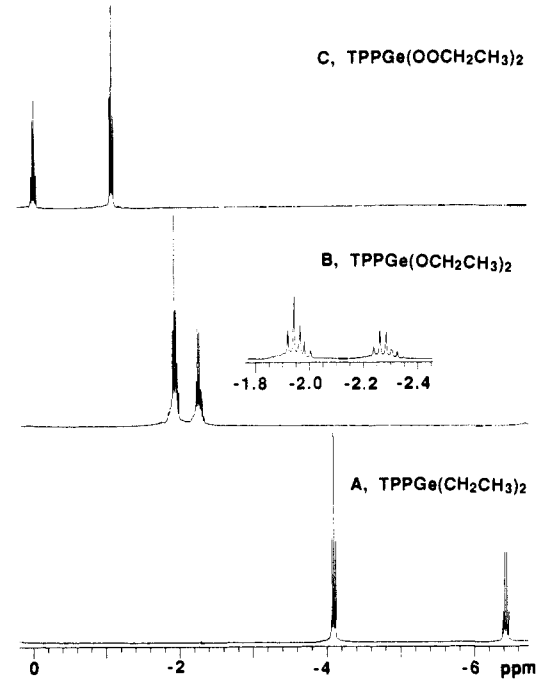

Figure 1. 300 MHz ^{1}H NMR spectra of benzene-d_8 solutions of (A) $TPPGe(CH_2CH_3)_2$, (B) $TPPGe(OCH_2CH_3)_2$, and (C) $TPPGe(OOCH_2CH_3)_2$.

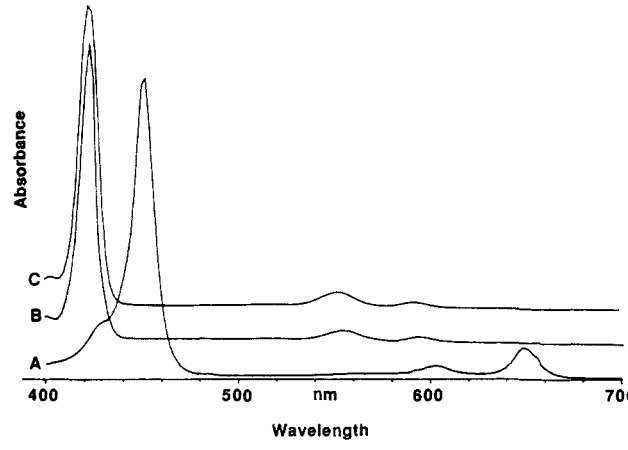

Figure 2. Electronic absorption spectra of (A) $TPPGe(CH_2CH_3)_2$, λ_{max}, nm ($\epsilon \times 10^{-3}$ cm^{-1} M^{-1}) 451 (315), 558 (7.2), 603 (15.4), 650 (39.0); (B) $TPPGe(OCH_2CH_3)_2$, λ_{max}, nm ($\epsilon \times 10^{-3}$ cm^{-1} M^{-1}) 426 (418), 517 (4.4), 556 (18.3), 595 (8.1); and (C) $TPPGe(OOCH_2CH_3)_2$, λ_{max}, nm ($\epsilon \times 10^{-3}$ cm^{-1} M^{-1}) 424 (594), 516 (3.8), 556 (20.8), 594 (8.9), in benzene solution.

$PGe(OR)_2$ (R = Ph, CH_3CO, and alkyl O), whereas less acidic substances, ethanol and *tert*-butyl alcohol, do not form appreciable quantities of the corresponding products. Thus treatment of a solution of $TPPGe(OH)_2$ with ethyl hydroperoxide yields $TPPGe(OOCH_2CH_3)_2$. $TPPGe(OOCMe_3)_2$ is obtained similarly. These reactions are of course the analogues of reactions for iron porphyrins that we have previously characterized. However, there is another important difference. TMPFeOH is a catalyst for the destruction of ethyl hydroperoxide,[3] but $TPPGe(OH)_2$ is not. Addition of catalytic amounts of $TPPGe(OH)_2$ to a benzene solution of ethyl hydroperoxide produces negligible change in the NMR spectrum of that solution after 10 h, whereas addition of an equivalent amount of TMPFeOH results in 80% conversion to acetaldehyde and ethanol after 5 min.

These germanium porphyrin complexes are most easily identified by their ^{1}H NMR spectra. Relevant data are collected in Table I. In particular the axial ligand resonances, which are subject to upfield shifts that result from ring current effects, are well-resolved and characteristic. The pyrrole resonances show

(9) (a) (Cumyl peroxo)pyridylbis(dimethylglyoximato)cobalt(III), O–O distance 1.455 (3) Å. Giannotti, C.; Fontaine, C.; Chiaroni, A.; Richie, C. *J. Organomet. Chem.* **1976**, *113*, 57. (b) 1-(*p*-Tolyl)(ethyl peroxo)(pyridylbis(dimethylglyoximato)cobalt(III), O–O distance, 1.455 (8) Å. Chiaroni, A., Pascard-Billy, C. *Bull. Soc. Chim. Fr.* **1973**, 781. (c) Peroxy *p*-quinalato complex of cobalt(III) with a pentadentate N_3O_2 Schiff-base, O–O distance, 1.50 (1) Å. Nishinaga, A.; Tomita, H.; Nishizawa, K.; Matsuura, T.; Ooi, S.; Hirotsu, K. *J. Chem. Soc., Dalton Trans.* **1981**, 1504. (d) $(\eta^5$-$C_5H_5)_2Hf(CH_2CH_3)(OOCMe_3)$, O–O distance, 1.489 (12) Å. van Asselt, A.; Santarsiero, B. D.; Bercaw, J. E. *J. Am. Chem. Soc.* **1986**, *108*, 8291. (e) $[(\mu$-$CCl_3CO_2)Pd^{II}(\mu$-$O_2Bu^t)]_4$, O–O distance, 1.49 Å. Mimoun, H.; Charpentier, R.; Mitschler, A.; Fischer, J.; Weiss, R. *J. Am. Chem. Soc.* **1980**, *102*, 1047. (f) (dipicolinato)V^V=O(η^2-O_2Bu^t), O–O distance, 1.436 (5) Å. Mimoun, H.; Chaumette, P.; Mignard, M.; Saussine, L.; Fischer, J.; Weiss, R. *Nouv. J. Chim.* **1983**, *7*, 467.

(10) Traylor, T. G.; Lee, W. A.; Stynes, D. V. *J. Am. Chem. Soc.* **1984**, *106*, 755. Gold, A.; Ivey, W.; Torey, G. E.; Sangaiah, R. *Inorg. Chem.* **1984**, *23*, 2932.

(11) (a) Cloutour, C.; La Farque, D.; Richards, J. A.; Pommier, J.-C. *J. Organomet. Chem.* **1977**, *137*, 157. (b) Cloutour, C.; La Farque, D.; Pommier, J. C. *J. Organomet. Chem.* **1980**, *190*, 35.

(12) Panek, E. J.; Whitesides, G. M. *J. Am. Chem. Soc.* **1972**, *94*, 8768. Blackburn, T. F.; Labinger, J. A.; Schwartz, J. *Tetrahedron Lett.* **1975**, *35*, 3041. Brindley, P. B.; Scotton, M. J. *J. Chem. Soc., Perkin Trans. II* **1981**, 419.

(13) Maskasky, J. E.; Kenney, M. E. *J. Am. Chem. Soc.* **1973**, *95*, 1443.

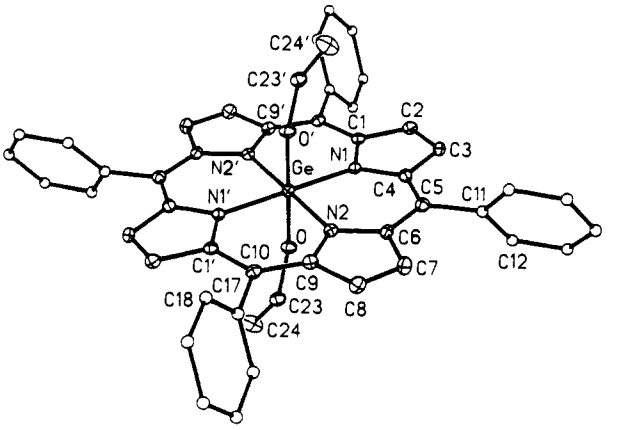

Figure 3. A perspective view of $TPPGe(OCH_2CH_3)_2$ as determined by X-ray diffraction.

only slight variations and are less informative. The phenyl resonances are also less useful. The upfield regions of the spectra of $TPPGe(CH_2CH_3)_2$, $TPPGe(OCH_2CH_3)_2$, and $TPPGe(OOCH_2CH_3)_2$ are shown in Figure 1. The resonances of the ethyl ligands in $TPPGe(CH_2CH_3)_2$ show the furthest upfield shift since these protons are held the closest to the porphyrin ring and experience the largest ring current. The resonances of the ethyl groups in the alkoxide and peroxide complexes show successively smaller shifts, since these groups are further from the porphyrin ring. Notice also that the positions of the methyl and methylene groups in $TPPGe(OOCH_2CH_3)_2$ are reversed from that seen in the ethoxy and ethyl complexes. This reversal results from two competing effects: the upfield ring current shift and the downfield shift due to the electronegativity of the oxygen substituent. While the H–H couplings within the alkoxide and peroxide complexes are similar, those of the ethyl complex are slightly (ca. 1 Hz) larger.

The electronic spectra of these complexes are less informative. The spectra of $TPPGe(CH_2CH_3)_2$, $TPPGe(OCH_2CH_3)_2$, and $TPPGe(OOCH_2CH_3)_2$ in solution are compared in Figure 2. The spectra of the latter two (and of $TPPGe(OH)_2$ which is not shown) are virtually identical, whereas that of the ethyl complex is different. In particular, the $TPPGe(CH_2CH_3)_2$ shows absorptions at lower energies than the complexes with oxygen-bound axial ligands.

The infrared spectra of these complexes are dominated by vibrations of the porphyrin ligands. However, careful comparison of the spectra of $TPPGe(OCH_2CH_3)_2$ and $TPPGe(OOCH_2CH_3)_2$ reveals the presence of a band at 835 cm^{-1} in the latter which has no counterpart in the spectrum of the former. This band is assigned to the peroxy O–O stretching frequency. This assignment is entirely consistent with other observations of peroxy O–O stretches.[14]

$TPPGe(OOCH_2CH_3)_2$ shows surprisingly good thermal stability in solution. NMR observations indicate that heating at 60 °C in benzene solution for 20 h results in negligible decomposition. However, the ethyl peroxide complex is sensitive to photolysis. Irradiation of a toluene solution of $TPPGe(OOCH_2CH_3)_2$ with visible light using a 638-nm filter causes the ^1H NMR resonances of the ethyl peroxide ligand to decay, while new resonances indicative of the formation of ethanol and acetaldehyde develop. At 23 °C the acetaldehyde/ethanol ratio is 0.55. A similar ratio is observed when the photolysis is conducted in benzene. However, when photolysis is conducted at −70 °C in toluene, that ratio is 3.5, and the products are formed much more slowly. The major germanium porphyrin product is $TPPGe(OH)_2$. However, two other pyrrole resonances are observed, and a number of small peaks develop in the region 7–5 ppm during photolysis. We suspect that these latter resonances arise from attack on the porphyrin ligand by radicals, particularly by the ethoxy radical, that are formed during decomposition of the axial ligands. $TPPGe(OCH_2CH_3)_2$ is not sensitive to photolysis under similar conditions.

$TPPGe(OOCH_2CH_3)_2$ is sensitive to hydrolysis. When water is added to a benzene solution of $TPPGe(OOCH_2CH_3)_2$, resonances due to $TPPGe(OH)_2$ and ethyl hydroperoxide develop. $TPPGe(OCH_2CH_3)_2$ is even more sensitive to hydrolysis, while $TPPGe(CH_2CH_3)_2$ is not.

The Structures of $TPPGe(OCH_2CH_3)_2$ and $TPPGe(OOCH_2CH_3)_2$. $TPPGe(OCH_2CH_3)_2$ crystallizes with one half-molecule of the complex in the asymmetric unit with no unusual contacts between these constituents. A drawing of the complex, which has crystallographically imposed inversion symmetry, is shown in Figure 3. Selected bond distances and angles are given in Table II. The germanium lies in the porphyrin plane with two axial

Table II. Selected Bond Distances (Å) and Angles (deg) for $TPPGe(OCH_2CH_3)_2$ and $TPPGe(OOCH_2CH_3)_2$

	$TPPGe(OCH_2CH_3)_2$	$TPPGe(OOCH_2CH_3)_2$ mol. A	$TPPGe(OOCH_2CH_3)_2$ mol. B
	Distances		
Ge–O	1.822 (2)	1.865 (3)	1.845 (3)
Ge–N(1)	2.024 (3)	2.023 (3)	2.029 (3)
Ge–N(2)	2.032 (3)	2.013 (3)	2.016 (3)
O–C	1.399 (5)	1.436 (4)	1.418 (17)
O–C	1.517 (6)	1.497 (6)	*a*
O–O		1.478 (6)	*a*
	Angles		
N(1)–Ge–O	87.8 (1)	87.8 (1)	92.5 (1)
N(2)–Ge–O	91.9 (1)	88.1 (1)	87.8 (1)
Gd–O–C(O)	126.4 (2)	110.4 (2)	121.5 (4)
O–C–C	109.6 (4)		
O–O–C		105.6 (2)	108.7 (7)

[a] Disordered.

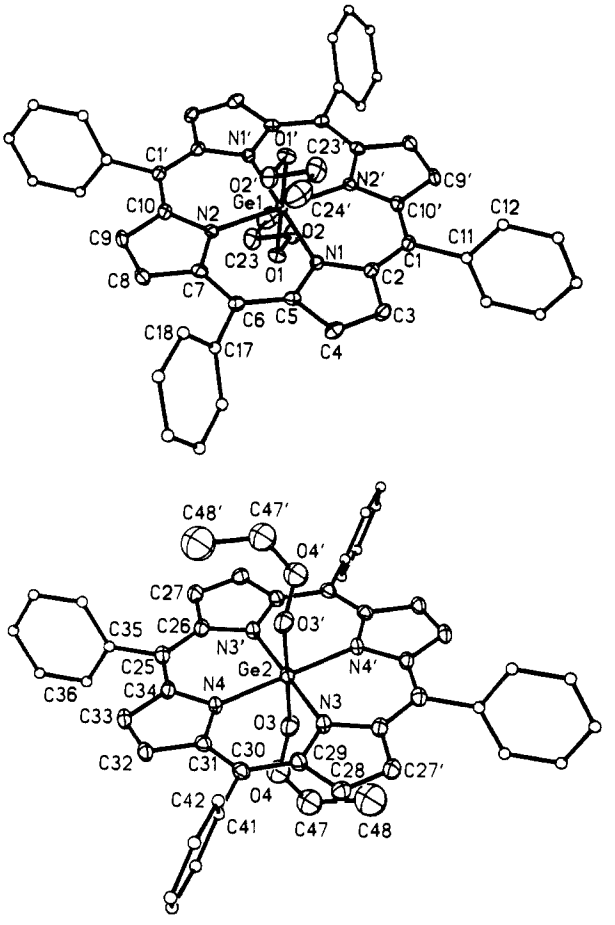

Figure 4. A perspective view of $TPPGe(OOCH_2CH_3)_2$: (top) the ordered molecule and (bottom) the molecule that shows disorder in the ethyl peroxide ligand with the principal form (54.8% occupancy) shown.

(14) *Sadtler Handbook of Infrared Spectra*; Simons, W. W., Ed.; Sadtler Research Laboratories: Philadelphia, PA, 1978; p 466.

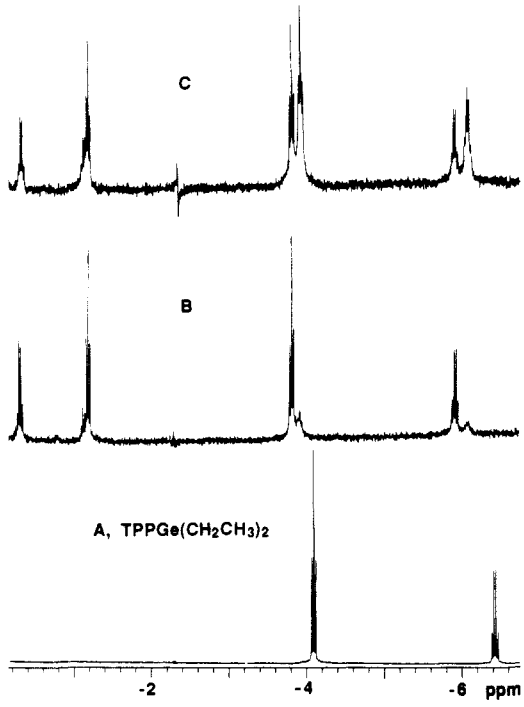

Figure 5. 300 MHz ^{1}H NMR spectra of the reaction of TPPGe(CH_2CH_3)$_2$ in benzene-d_6 solution with dioxygen (A) before irradiation, (B) after irradiation (cut off filter at 638 nm); and (C) the same sample after shaking with water.

ethoxide ligands that complete the octahedral-like geometry.

TPPGe($OOCH_2CH_3$)$_2$ crystallizes with two independent half-molecules of the complex in the asymmetric unit. There are no unusual interactions between these. Drawings of the two forms of the complex are presented in Figure 4. Both have six-coordinate germanium and inversion symmetry like that seen in the ethoxide complex. The two forms differ principally in the arrangement of the atoms within the ethyl peroxide ligands. In form A the oxygen and carbon atoms are arranged in a planar zigzag array that is common for hydrocarbon fragments. In form B the O_2C_2 unit is nonplanar, and the position of the terminal carbon atom is disordered. Because of this disorder, the dimensions within the ethyl peroxide ligand in the B form are less accurately determined than in the A form. The figure shows the orientation of the more prevalent (54.8%) arrangement of the peroxide in the B form. In this, the ethyl peroxide ligand spirals out from the germanium atom. The dimensions of the ethoxide and ethyl peroxide complex may be compared by turning to Table II. Overall the two structures are highly comparable and similar to that of (dihydroxyporphinato)germanium(IV).[15] The Ge–N distances are similar and similar to those in other germanium(IV) porphyrins.[15,16] The Ge–O distances are considerably shorter than the Ge–N distances but are consistent with those found in other germanium(IV) compounds having oxygen donors.[15,17] The O–O distance in the ethyl peroxide complex is consistent with corresponding distances in other alkyl peroxide complexes[9] and organic peroxides.[19]

The Reaction of TPPGe(CH_2CH_3)$_2$ with Dioxygen. In solution the ethyl complex is unaffected by dioxygen as long as the sample is handled in the dark. This contrasts with the iron(III) alkylporphyrin complexes which react rapidly with dioxygen even at −80 °C in the dark.

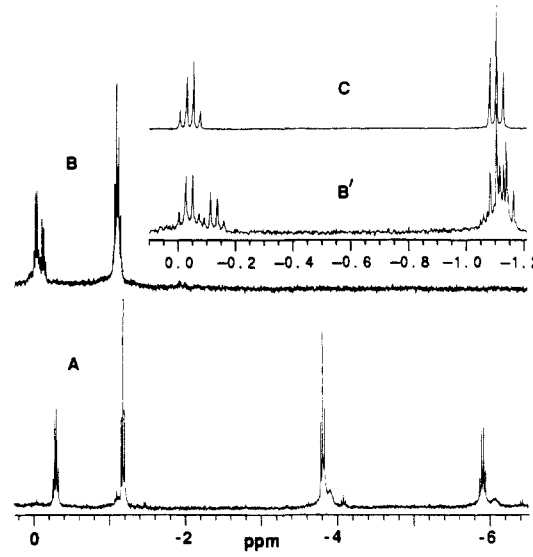

Figure 6. ^{1}H NMR spectra of the further photolysis of a benzene-d_6 solution of TPPGe($OOCH_2CH_3$)(CH_2CH_3) in the presence of dioxygen (A) before irradiation, (B) after irradiation (cut off filter at 515 nm), (B′) expansion of the 0 to −1.2 ppm region of (B); and (C) 0 to −1.2 ppm region for TPPGe($OOCH_2CH_3$)$_2$.

Figure 5 shows the effect of photolysis in the upfield region of the ^{1}H NMR spectrum where axial ligand resonances occur. Trace A shows the spectrum of TPPGe(CH_2CH_3)$_2$ in benzene-d_6 before photolysis, while trace B shows the effect of selective irradiation at $\lambda > 638$ nm with a solution that is saturated with dioxygen. These are the conditions developed by Cloutour, La Farque, and Pommier.[11] Upon photolysis the resonances due to the diethyl compound decrease in intensity, and four new sets of resonances develop. Resonances at −3.8 and −5.8 ppm are due to a coordinated ethyl group, while those at −0.2 and −1.2 ppm are assigned to a coordinated ethyl peroxide ligand. Notice that the latter are in the same region as the axial ligand resonances in TPPGe($OOCH_2CH_3$)$_2$. They appear at distinctly lower field than would be expected for a coordinated ethoxide. The integrated intensities of the resonances for the ethyl and ethyl peroxide ligands are 1:1. Thus the initial photolysis product is TPPGe($OOCH_2CH_3$)(CH_2CH_3). Previous work, at lower field, reported only a broad feature between −0.48 and −0.81 for the presumed ethyl peroxide ligand.[11] No data were presented to differentiate this from an ethoxide ligand, nor were the effects of hydrolysis (vide infra) described. Treatment of TPPGe($OOCH_2CH_3$)(CH_2CH_3) with water results in the hydrolysis of the ethyl peroxide ligand but not the ethyl ligand. As seen in trace C of Figure 5, resonances at 3.9 and 6.1 ppm due to TPPGe(CH_2CH_3)(OH) grow into the spectrum. At this stage resonances due to ethyl hydroperoxide, the other hydrolysis product, have developed at lower field (not shown).

This process offers a unique pathway for selective formation of germanium porphyrins with two different axial ligands. In another example, treatment of a sample of TPPGe($OOCH_2CH_3$)(CH_2CH_3) with hydrogen chloride produces ^{1}H NMR resonances consistent with the formation of ethyl hydroperoxide and TPPGeCl(CH_2CH_3) (data in Table I). Notice, however, that the coupling constant seen in the ethyl group is smaller than anticipated. This procedure also allows for the preparation and spectroscopic identification of an η'-hydroperoxide complex. Treating a benzene-d_6 solution of TPPGe($OOCH_2CH_3$)(CH_2CH_3) with a benzene-d_6 solution which had been shaken with 30% aqueous hydrogen peroxide results in the loss of the ^{1}H NMR resonances of the ethyl peroxide ligand and the upfield shift of the ethyl resonances (see Table I). These resonances appear in a different position from those of TPPGe(OH)(CH_2CH_3) and are consequently assigned to TPPGe(OOH)(CH_2CH_3). In this case, the unique sensitivity of the ring current shifted ethyl resonance allows spectroscopic inference for the existence of a ligand that is otherwise rather difficult to detect.

(15) Mavridis, A.; Tulinksy, A. *Inorg. Chem.* **1976**, *15*, 2723.
(16) Miyamoto, T. K.; Sugita, N.; Matsumoto, Y.; Sasaki, Y.; Konno, M. *Chem. Lett.* **1983**, 1695. Guilard, R.; Barbe, J.-M.; Boukhris, M.; Lecomte, C. *J. Chem. Soc. Dalton Trans.* **1988**, 1921. Guilard, R.; Barbe, J.-M.; Boukhris, A.; Lecomte, C.; Anderson, J. E.; Xu, Q. Y.; Kadish, K. M. *J. Chem. Soc., Dalton Trans.* **1988**, 1109.
(17) Day, R. O.; Holmes, J. M.; San, A. C.; Holmes, R. R. *Inorg. Chem.* **1982**, *21*, 281. San, A. C.; Day, R. O.; Holmes, R. R. *J. Am. Chem. Soc.* **1980**, *102*, 7972.

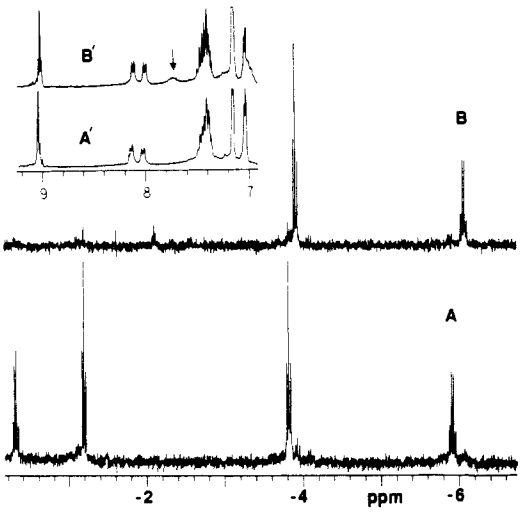

Figure 7. ^1H NMR spectra showing the reaction of triphenylphosphine with TPPGe($OOCH_2CH_3$)(CH_2CH_3) (A) before reaction and (B) after reaction. Inserts A′ and B′ show the phenyl region, and the arrow indicates the position of the triphenylphosphine oxide resonance.

Photolysis of TPPGe(CH_2CH_3)$_2$ and of TPPGe($OOCH_2CH_3$)(CH_2CH_3) with a cut off filter at higher energies ($\lambda > 498$ nm) results in the formation of additional photoproducts that result from the involvement of both ethyl ligands. Figure 6 shows the effect of such irradiation on TPPGe($OOCH_2CH_3$)(CH_2CH_3). The upfield region of the ^1H NMR spectrum after irradiation reveals that the resonances of TPPGe($OOCH_2CH_3$)(CH_2CH_3) are lost but that two sets of resonances are present in the region characteristic of ethyl peroxide ligands. One set is due to TPPGe($OOCH_2CH_3$)$_2$, which has been independently prepared. This is best verified by examining the inset B′ and C. Inset C shows the spectrum of pure TPPGe($OOCH_2CH_3$)$_2$. The second set is ascribed to TPPGe($OOCH_2CH_3$)OH, a product of partial hydrolysis of TPPGe($OOCH_2CH_3$)$_2$. It too has been independently observed. This mixed ligand complex forms in solutions of TPPGe($OOCH_2CH_3$)$_2$ which have been exposed to limited amounts of water.

The need for higher energy light for the formation of TPPGe($OOCH_2CH_3$)$_2$ by photolysis stems from the systematic shift in electronic spectra that accompanies the successive transformation of carbon-bound ethyl ligands into oxygen-bound ethyl peroxide ligands. Thus TPPGe($OOCH_2CH_3$)(CH_2CH_3) has absorption features at 440 nm (Soret), 576, and 618. These features fall in between those of TPPGe(CH_2CH_3)$_2$ and TPPGe($OOCH_2CH_3$)$_2$ that are shown in Figure 2. They are also similar to the spectral features seen for another mixed ligand complex, TPPGeCl(Ph): λ_{max}, 439 (Soret), 574, and 616 nm.[18]

The reactivity of TPPGe($OOCH_2CH_3$)(CH_2CH_3) toward a good oxygen atom acceptor, triphenylphosphine, has been examined. The results are shown in Figure 7. Trace A shows the spectrum of a sample of the mixed axial ligand complex obtained as described above, while trace B shows the effect of the addition of triphenylphosphine. In the latter the resonances of the ethyl peroxide ligand have been lost, and those of the ethyl ligand have moved to slightly higher field which is consistent with the formation of TPPGe(OH)(CH_2CH_3). At lower field the spectrum reveals that triphenylphosphine oxide (see insert) and ethanol (not shown) are formed. The resonance of the triphenylphosphine oxide is broadened due to hydrogen bonding with the GeOH group. The reaction probably proceeds through the formation of an ethoxy complex that is readily hydrolyzed by the traces of water present.

Discussion

The major chemical transformations encountered in this work are summarized in Scheme I. TPPGe($OOCH_2CH_3$)$_2$ represents the first porphyrin complex of any metal bearing an alkyl peroxide

Scheme I

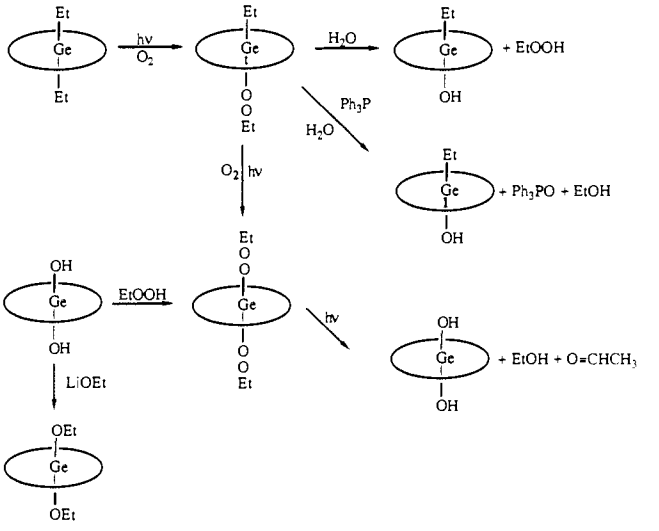

axial ligand to be structurally characterized.[26] Of the other alkyl peroxide structures, only one[9b] involves a hydroperoxide that is not stabilized by having a tertiary carbon bound to the peroxy groups. The stability of this germanium ethyl peroxide complex and the fact that the crystalline sample used for the diffraction study was obtained in the presence of excess ethyl hydroperoxide emphasizes the fact that alkyl hydroperoxides themselves are not responsible for the porphyrin degradation[10] that frequently accompanies metalloporphyrin catalyzed hydroperoxide reactions. Rather, reactive products (probably alkoxyl radicals) that are generated in the alkyl hydroperoxide/metalloporphyrin reaction cause attack on the porphyrin core. The stability of TPPGe($OOCH_2CH_3$)$_2$ also indicates that simple coordination of a Lewis acid metal ion to the alkyl peroxide is not sufficient to initiate its decomposition. This observation, which is consistent with previous observation of the effects of Lewis acids on alkyl peroxides, strongly suggests that the iron porphyrin catalyzed decomposition of alkyl peroxides necessitates oxidation of the iron porphyrin complex to a ferryl, $(Fe^{IV}{=}O)^{2+}$, form.

The formation of ethyl peroxide ligands by photolysis of the ethyl compound appears to involve homolysis of the Ge–C bonds and subsequent reaction of the ethyl radicals with dioxygen as shown in eq 6. Precedent for homolysis of metal–carbon bonds

$$\mathrm{Ge{-}CH_2CH_3} \xrightarrow{h\nu} \mathrm{Ge^{\bullet}} + {}^{\bullet}\mathrm{CH_2CH_3} \qquad \mathrm{Ge^{\bullet}} \xrightarrow{O_2} \mathrm{GeOOCH_2CH_3} + {}^{\bullet}\mathrm{OOCH_2CH_3} \qquad (6)$$

during photolysis of metalloporphyrins comes from extensive work on cobalt(III) complexes,[20] observations on indium(III) porphyrins,[21] our earlier studies of iron(III) porphyrins,[3] and photolysis of OEPGePh_2 (OEP is the dianion of octaethylporphyrin) in chloroform.[22]

The photolysis of TPPGe($OOCH_2CH_3$)$_2$ presumably occurs by homolysis of the O–O bond according to eq 7. Two products,

(18) Xu, Q. Y.; Barbe, J.-M.; Kadish, K. M. *Inorg. Chem.* **1988**, *27*, 2373.

(19) Silbert, L. S. In *Organic Peroxides*; Swern, D., Ed.; Wiley: New York, 1971; Vol. 2, p 649. Numan, H.; Wieringa, J. H.; Wynberg, H.; Hess, J.; Vos, A. *J. Chem. Soc., Chem. Commun.* **1977**, 591. Groth, P. *Acta Chem. Scand* **1970**, *24*, 2137. Wilson, R. M.; Gardner, E. J.; Elder, R. C.; Squire, R. H.; Florian, L. R. *J. Am. Chem. Soc.* **1974**, *96*, 2955. Jeffrey, J.; Mawky, R. J.; Hursthouse, M. B.; Walker, N. P. C. *J. Chem. Soc., Chem. Commun.* **1982**, 1411.

(20) Toscano, P. J.; Marzilli, L. G. *Prog. Inorg. Chem.* **1984**, *31*, 105. Denaiu, J.; Gaudemer, A. J. *Organomet. Chem.* **1980**, *191*, C1.

(21) Hoshino, M.; Ida, H.; Yasufuku, K.; Tanaka, K. *J. Phys. Chem.* **1986**, *17*, 3984. Hoshino, M.; Yamaji, M.; Hama, Y. *Chem. Phys. Lett.* **1986**, *125*, 369.

(22) Kadish, K. M.; Xu, Q. Y.; Barbe, J.-M.; Anderson, J. E.; Wang, E.; Guilard, R. *J. Am. Chem. Soc.* **1987**, *109*, 7705.

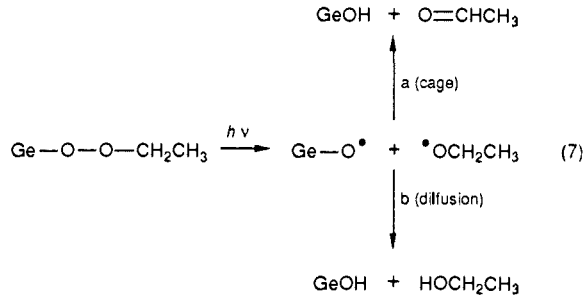

acetaldehyde and ethanol, can form depending on the subsequent reactions of the ethoxy radical. If the ethoxy radical is oxidized by the Ge–O• unit before it diffuses away from the porphyrin complex, then acetaldehyde is formed (path a). However, if the Ge–O• and ethoxy radical diffuse apart, hydrogen atom abstraction from the medium can yield ethanol as the organic product. The ratio of acetaldehyde-to-ethanol is smaller in the photolytic decomposition of TPPGe($OOCH_2CH_3$)$_2$ in toluene at 25 °C than at −70 °C. This is consistent with eq 7 since diffusion out of the cage, which favors ethanol formation, is expected to be greater at the higher temperature. The fact that the acetaldehyde/ethanol ratio is the same in benzene and toluene also suggest that diffusion rather than the hydrogen atom availability from solvent governs the product ratio. Notice, however, that the acetaldehyde/ethanol ratio is much higher for the thermal decomposition of PFeOOCH_2CH_3 (ratio 24).[3] This may result from a difference in intrinsic reactivities of the PFeO vs the PGeO($OOCH_2CH_3$) fragments that are formed upon O–O bond homolysis. The PFeO fragment must be much more prone to hydrogen atom abstraction.

Experimental Section

Preparation of Compounds. TTPGeCl_2,[13] TPPGe$(OH)_2$,[13] TPPGe(C$H_2CH_3)_2$,[13] and ethyl hydroperoxide[23] were prepared according to established routes. TPPGe$(CH_2CH_3)_2$ was manipulated under reduced lighting.

TPPGe($OOCH_2CH_3$)$_2$. A solution of ethyl hydroperoxide in ether was added to 60 mg of TPPGe$(OH)_2$ dissolved in 50 mL of dichloromethane in a darkened room. After stirring for 5 min, the solvent was removed under vacuum with the use of a rotary evaporator to yield 62 mg (92%) of a purple powder. Analysis by ^{1}H NMR shows that the sample is free of other porphyrin-containing impurities. Crystals suitable for X-ray diffraction were obtained by diffusion of a 10% (by volume) solution of ethyl hydroperoxide in ether into a benzene solution of the complex which was protected from exposure to light. The complex reacts with chlorinated solvents to form TPPGeCl_2.

TPPGe(OCH_2CH_3)$_2$. A solution of *tert*-butyllithium (2.4 mL of a 1.1 M solution in hexane) was added to a solution of ethanol (10 mL, 220 mmol, distilled from magnesium turnings) in 50 mL of diethyl ether (distilled from sodium/potassium amalgam) at −78 °C. After completion of the addition the solution was warmed to room temperature and added via a cannula to a solution of 98 mg (0.13 mmol) of TPPGeCl_2 in 50 mL of benzene (distilled from sodium). The mixture was heated under reflux until all of the TPPGeCl_2 (monitored at the Soret band at 430 nm) was converted to product (Soret at 424 nm). This took less than 30 min. The solvent was then removed by vacuum distillation. The solid was recrystallized from dichloromethane/hexane to give 88 mg (0.113 mmol, 87%) of fine purple crystals of TPPGe$(OCH_2CH_3)_2$. The sample is not sensitive to exposure to light.

Photolysis Studies. Photolysis involved irradiation of samples contained in 5-mm NMR tubes using light from a 60-W tungsten bulb. The tubes did not suffer appreciable warming during photolysis. A Newport RG 645 filter was used to exclude light at wavelengths less than 638 nm, and a RG 515 filter was used to exclude light at wavelengths less than 498 nm.

Instrumentation. ^{1}H NMR spectra were recorded at 300 MHz on a General Electric QE 300 Fourier transform spectrometer. Electronic spectra were obtained by using a Hewlett Packard 9122 diode array spectrometer, and infrared spectra were obtained with Nujol mulls by using an IBM IR32 infrared spectrometer.

X-ray Crystallographic Studies. TPPGe(OCH_2CH_3)$_2$. A suitable crystal was mounted on a glass fiber by using silicone grease and positioned in the cold stream of the X-ray diffractometer. Only random fluctuations (<2%) in the intensities of two standard reflections were observed during the course of data collection. Crystal data are given in Table III.

Table III. Crystal Data, Data Collection, and Structure Solution Parameters for TPPGe($OOCH_2CH_3$)$_2$ and TPPGe(OCH_2CH_3)$_2$

	TPPGe($OOCH_2CH_3$)$_2$	TPPGe(OCH_2CH_3)$_2$
formula	$C_{48}H_{38}GeN_4O_4$	$C_{48}H_{38}GeN_4O_2$
fw	807.45	775.90
color and habit	magneta plates	red-violet parallelepipeds
crystal system	triclinic	monoclinic
space group	$P\bar{1}$	$P2_1/c$
a, Å	10.941 (1)	9.745 (2)
b, Å	11.212 (1)	15.350 (3)
c, Å	17.015 (2)	13.084 (3)
α, deg	89.53 (1)	
β, deg	73.77 (1)	107.65 (2)
γ, deg	70.78 (1)	
V, Å^3	1884.3 (4)	1865.1 (7)
T, deg	130 K	130 K
Z	2	2
cryst dimens, mm	0.23 × 0.33 × 0.50	0.40 × 0.40 × 0.60
d_{calcd}, g cm^{-3}	1.42	1.38
radiation, Å)	Mo Kα, (λ = 0.71069)	Mo Kα, (λ = 0.71069)
μ(Mo Kα), cm^{-1}	9.07	9.2
range of transmission factors	0.74–0.85	0.67–0.74
diffractometer		
scan method	ω, 1.2° range, 1.0° offset for bkgnd	ω, 1.1° range, 1.0° offset for bkgnd
scan speed, deg min^{-1}	10	60.0
2° range, deg	0–50	0–50
octants collected	$h\pm k,\pm l$	$h,k,\pm l$
no. data collected	6642	3635
no. unique data	6642	3287 [R(merge) = 0.010]
no. data used in refinement	5200 [$I > 2\sigma(I)$]	2508 [$I > 2\sigma(I)$]
no. params refined	518	252
R^a	0.044	0.044
$R_w{}^a$	0.048 [$w = 1/\sigma^2(F_o)$]	0.043 [$w = 1/\sigma^2(F_o)$]

$^a R = \sum||F_o| - |F_c||/|F_o|$ and $R_w = \sum||F_o| - |F_c||w^{1/2}/\sum|F_o w^{1/2}|$.

The usual corrections for Lorentz and polarization effects were applied to the data. Crystallographic programs used were those of SHELXTL, version 5, installed on a Data General Eclipse computer. Scattering factors and corrections for anomalous dispersion were from the *International Tables*.[24]

The structure was solved by direct methods. The ethyl group of the ethoxide suffered from disorder and was modeled with 0.81 occupancy for C(23A) and C(24A) and 0.19 occupancy for the corresponding "B" atoms. The "B" atoms were located on difference maps, and their positions were fixed during refinement. An absorption correction was applied.[25] Final refinement was carried out with anisotropic thermal parameters for all non-hydrogen atoms except the minor form of the ethyl group. Hydrogen atoms were included at calculated positions by using a riding model, with C–H of 0.96 Å and U_H = 1.2 U_C (hydrogens on C(23A) and C(24A) were located on a difference map and included in the structure factor calculation without refinement). No features larger than 0.35 e Å^{-3} appeared on the final difference map. The largest shift in the final cycle of refinement was 0.006 for U_{12} of C(7).

TPPGe($OOCH_2CH_3$)$_2$. Although the crystals decompose upon removal from the mother liquor, their crystallinity could be preserved for hours by immersing them still wet in a hydrocarbon oil. The crystal selected for data collection was a well-formed plate. It was mounted on a glass fiber by using silicone grease and positioned in the cold stream of the X-ray diffractometer. Only random fluctuations of less than 2% in the intensities of two standard reflections were observed during the course of data collection. The data were handled as described for TPPGe(OCH_2CH_3)$_2$. Crystal data are given in Table III.

The structure was solved by Patterson methods. There are two half-molecules in the asymmetric unit. Full molecules are generated by the inversion operation. One of the two molecules is completely ordered; the other has disorder in the position of the ethyl peroxide group. There

(23) Williams, Rh. R.; Mosher, H. S. *J. Am. Chem. Soc.* **1954**, *76*, 2984.

(24) *International Tables for X-ray Crystallography*; Kynoch Press: Birmingham, England, 1974; Vol. 4.

(25) The Program XABS which obtains an absorption tensor from $F_o - F_c$ differences was used: Moezzi, B. Ph.D. Dissertation, University of California, Davis, CA.

(26) **Note Added In Proof**: In the period since this was written, the preparation and structure of TPPCo^{III}OOCH_2CH=CH_2 have been reported: Mikolaiski, W.; Baum, G.; Massa, W.; Hoffmann, R. W. *J. Organomet. Chem.* **1989**, *376*, 397.

are two possible orientations for this group, with refined group occupancies of 54.8 (5)% for the "B" form and 45.2 (5)% for the "A" form.

An absorption correction was applied.[25] Final refinement was carried out with anisotropic thermal parameters for all non-hydrogen atoms that were not disordered. Hydrogen atoms were included at calculated positions with use of a riding model except for those bonded to the disordered ethyl carbons. Isotropic thermal parameters for the hydrogen atoms were fixed at 1.2 times that of the bonded carbon. The largest peak in a final difference map had a value of 0.69 e $Å^{-3}$ and is located near the disordered ethyl peroxide.

Acknowledgment. We thank the National Institutes of Health (GM 26226) for financial support.

Supplementary Material Available: Table of atomic coordinates, bond lengths, bond angles, hydrogen atom positions, and anisotropic thermal parameters for $TPPGe(OCH_2CH_3)_2$ and $TPPGe(OOCH_2CH_3)_2$ (18 pages); tables of observed and calculated structure factors for these two complexes (46 pages). Ordering information is given on any current masthead page.

Synthetic Design of a Multielectron Series of Homologous Dirhodium Fluorophosphines Possessing an Emissive $d\sigma^*$ Excited State

Joel I. Dulebohn, Donald L. Ward, and Daniel G. Nocera*,†

Contribution from the Department of Chemistry and the LASER Laboratory, Michigan State University, East Lansing, Michigan 48824. *Received August 3, 1989*

Abstract: A novel homologous series of $Rh_2(0,0)$, $Rh_2(0,II)$, and $Rh_2(II,II)$ bis(difluorophosphino)methylamine complexes have been synthesized and structurally and electronically characterized. These binuclear rhodium compounds are all prepared from the reaction of $[RhCl(PF_3)_2]_2$ with $CH_3N(PF_2)_2$. Under reducing conditions, $Rh_2[CH_3N(PF_2)_2]_3(PF_3)_2$ (**1**) is isolated in moderate yields. Orange crystals of **1**, prepared by layering hexane over a dichloromethane solution of **1**, are triclinic with a space group $P\bar{1}$, $a = 10.021$ (4) Å, $b = 10.139$ (4) Å, $c = 14.299$ (7) Å, $\alpha = 74.95$ (3)°, $\beta = 76.79$ (3)°, $\gamma = 62.17$ (3)°, $V = 1230.9$ (9) $Å^3$, and $Z = 2$. The structure was refined to $R = 0.067$ and $R_w = 0.078$. Conversely, reaction of $[RhCl(PF_3)_2]_2$ with $CH_3N(PF_2)_2$ in the presence of the oxidant $Cl_2IC_6H_5$ produces $Rh_2[CH_3N(PF_2)_2]_3Cl_4$ (**3**) in high yields. Yellow needles of **3**, obtained from an ether–THF solution, are monoclinic with a space group $C2/c$; the cell parameters are $a = 15.462$ (2) Å, $b = 10.999$ (2) Å, $c = 14.256$ (2) Å, $\beta = 107.52$ (1)°, $V = 2312.0$ (6) $Å^3$, and $Z = 4$. Compound **3** contains a crystallographic C_2 axis. After refinement $R = 0.042$ and $R_w = 0.045$. In the absence of oxidants and reductants, the unsymmetrical mixed-valence $Rh_2[CH_3N(PF_2)_2]_3Cl_2(PF_3)$ (**2**) complex is obtained. The molecular structure of **2** is a composite of **1** and **3** in that the trigonal-bipyramidal coordination geometry about Rh(0) centers in **1** and the octahedral coordination at the Rh(II) centers in **3** are retained about the mixed-valence $Rh_2(0,II)$ core. For each complex the ligands are rotated considerably from an eclipsed conformation. The Rh···Rh separations of 2.841 (2), 2.785 (1), and 2.707 (1) Å in **1**, **2**, and **3**, respectively, are consistent with the presence of a Rh–Rh single bond. Electronic structural considerations suggest that the metal–metal bond results from the overlap of the one-electron-occupied d_{z^2} orbitals of rhodium centers. Accordingly, **1**, **2**, and **3** comprise an electronically related series best represented as $(d^8)d^1$–$d^1(d^8)$, $(d^8)d^1$–$d^1(d^6)$, and $(d^6)d^1$–$d^1(d^6)$, respectively. Electronic absorption spectra are dominated by intense bands, which are characteristic of $\sigma \rightarrow d\sigma^*$ transitions. Crystalline solids of **1**, **2**, and **3** exhibit red, long-lived emissions ($\tau = 53$, 79, and 287 μs, respectively) upon excitation with frequencies coincident with the absorption manifold. Luminescence is consistent with a $d\sigma^*$ excited-state parentage of primarily triplet character.

Transition-metal complexes in electronic excited states can exhibit unique chemical reactivity. Whereas some excited-state processes follow dissociative reaction pathways, many transition-metal complexes exist as discrete molecular species in thermally equilibrated excited states.[1-4] For the latter case, the thermodynamic driving force for the reaction exceeds that of the ground state by an amount comparable to the internal energy of the excited state. This increased driving force is oftentimes manifested in the excited state overcoming large thermodynamic and/or kinetic barriers confronting the corresponding ground-state species. A central theme of inorganic photochemistry has been to exploit these thermodynamic and kinetic enhancements to promote novel oxidation–reduction reactions.[5-11] Because many important reactions involve multielectron transformations, recent attention has been focused on developing photochemical schemes in which the photoreagent effects a multielectron process. Although guidelines for multielectron photoreactivity have begun to emerge,[12-16] few photochemical schemes have been realized in which the initial multielectron photoreagent is regenerated.[17,18] As is the case for the photoreactant, the multielectron photoproduct typically resides in deep thermodynamic or kinetic wells that hinder its conversion back to the desired photoreactive state.

† Alfred P. Sloan Fellow and NSF Presidential Young Investigator.

(1) Juris, A.; Balzani, V.; Barigelletti, F.; Campagna, S.; Belser, P.; von Zelewsky, A. *Coord. Chem. Rev.* **1988**, *84*, 85-277.
(2) *Photochemistry and Photophysics of Coordination Compounds*; Yersin, H., Vogler, A., Eds.; Springer-Verlag: Berlin, 1987.
(3) Adamson, A. W. *J. Chem. Educ.* **1983**, *60*, 797-802.
(4) Porter, G. B. In *Concepts of Inorganic Photochemistry*; Adamson, A. W., Fleischauer, P. D., Eds.; Wiley: New York, 1975.
(5) *Photoinduced Electron Transfer*; Fox, M. A., Chanon, M., Eds.; Elsevier: Amsterdam, 1988; Part D.
(6) Meyer, T. J. *Acc. Chem. Res.* **1989**, *22*, 163-170.
(7) Kavarnos, G. J.; Turro, N. J. *Chem. Rev.* **1986**, *86*, 401-449.
(8) Balzani, V.; Sabbatini, N.; Scandola, F. *Chem. Rev.* **1986**, *86*, 319-337.
(9) *Energy Resources through Photochemistry and Catalysis*; Grätzel, M., Ed.; Academic Press: New York, 1983.
(10) Gray, H. B.; Maverick, A. W. *Science* **1981**, *214*, 1201-1205.
(11) *Photochemical Conversion and Storage of Solar Energy*; Connolly, J. S., Ed.; Academic Press: New York, 1981.
(12) (a) Roundhill, D. M.; Gray, H. B.; Che, C.-M. *Acc. Chem. Res.* **1989**, *22*, 55-61. (b) Marshall, J. L.; Steigman, A. E.; Gray, H. B. In *Excited States and Reactive Intermediates*; Lever, A. B. P., Ed.; ACS Symposium Series 307; American Chemical Society: Washington, DC, 1986; pp 166-176 and references therein. (c) Caspar, J. V.; Gray, H. B. *J. Am. Chem. Soc.* **1984**, *106*, 3029-3030.

0002-7863/90/1512-2969$02.50/0